Theoretical study of the CO catalytic oxidation on Au/SAPO-11 zeolite

ARTICLE *in* INTERNATIONAL JOURNAL OF QUANTUM CHEMISTRY · JULY 2010

Impact Factor: 1.43 · DOI: 10.1002/qua.22718

3 AUTHORS:

Beulah Griffe
Venezuelan Institute for Scientific Research
50 PUBLICATIONS **58** CITATIONS
SEE PROFILE

Anibal Sierraalta
Venezuelan Institute for Scientific Research
94 PUBLICATIONS **794** CITATIONS
SEE PROFILE

Joaquin L Brito
Venezuelan Institute for Scientific Research
186 PUBLICATIONS **1,366** CITATIONS
SEE PROFILE

Theoretical Study of the CO Catalytic Oxidation on Au/SAPO-11 Zeolite

BEULAH GRIFFE,[1] ANIBAL SIERRAALTA,[2] JOAQUÍN L. BRITO[1]

[1]*Laboratorio de Fisico-Química de Superficies, Centro de Química, IVIC, Apdo. Postal 20632, Caracas 1020-A, Venezuela*

[2]*Laboratorio de Química Computacional, Centro de Química, IVIC, Apdo. Postal 20632, Caracas 1020-A, Venezuela*

Received 11 February 2010; accepted 3 March 2010
Published online 8 July 2010 in Wiley InterScience (www.interscience.wiley.com).
DOI 10.1002/qua.22718

ABSTRACT: Quantum chemistry calculations were carried out, using ONIOM2 methodology, to investigate the CO adsorption and oxidation on gold supported on Silicoaluminophospates (SAPO) molecular sieves Au/SAPO-11 catalysts. Two models were studied, one containing one Au atom per site (Au—SAPO-11), and the other with two Au atoms per site (Au_2—SAPO-11). The results reveal that the CO adsorption and oxidation are exothermic on Au/SAPO11 with an ΔE of -41.0 kcal/mol and $\Delta E = -52.0$ kcal/mol, for the adsorption and oxidation, respectively. On the Au_2—SAPO-11 model, the CO adsorption and oxidation reaction occur, with a ΔE of -29.7 kcal/mol and -52 kcal/mol, respectively. According to our results, the oxidation reaction exhibits an Eley-Rideal type mechanism with adsorbed CO. The theoretical calculations reveal that this type of material could be interesting to disperse Au and consequently to strengthen its catalytic use for different reactions.
Int J Quantum Chem 110: 2573–2582, 2010

Key words: quantum chemistry; ONIOM; CO adsorption; Au—SAPO; theoretical; calculations

1. Introduction

As Haruta et al. [1] reported that gold catalytic behavior depends markedly on the type of support, degree of dispersion, and preparation method, the Au research about its use as catalyst has become of great importance and relevance. When gold is deposited on selected metal oxides as hemispherical ultrafine particles with diameters < 5 nm, it exhibits surprisingly high-activity and/or selectivity for such reactions as CO and saturated hydrocarbons combustion, amines and organic halogenated compounds oxidation-decomposition, hydrocarbons partial oxidation, the hydrogenation of carbon oxides, unsaturated carbonyl compounds, alkynes and dienes, and the reduction of nitrogen oxides [2, 3]. Recently, Au

Correspondence to: B. Griffe; e-mail: beulah.griffe@gmail.com

has attracted much attention, not only in heterogeneous catalysis but also in colloidal chemistry and nano-components manufacture, and in some other applications [4].

The most studied reaction using gold nano-particles is CO oxidation at low-temperatures [1, 5]. This focus on CO oxidation is because of its potential for practical applications such as, in the purification of feeds for automobile hydrogen fuel cells, (as CO poisons the fuel cell catalysts) and because CO presents advantages for fundamental understanding by being a good probe of catalyst surface structures [6]. Recently Hu and coworkers published a review on the advances on the modeling of CO oxidation with Au nano-particles, using DFT [7]. In this review article, two reaction mechanisms for CO oxidation have been proposed: an Eley-Rideal mechanism (E-R) on nonactive supporting materials (MgO) [8, 9] and a Langmuir-Hinshelwood mechanism (L-H) on active supporting materials (TiO_2) [10]. However, Shiga and Haruta [11] mentioned four mechanisms: (a) adsorbed CO and gaseous O_2 (E-R mechanism), (b) adsorbed O_2 and gaseous CO (E-R mechanism), (c) adsorbed CO and vicinally adsorbed O_2 (L-H mechanism), and (d) adsorbed CO and geminally adsorbed O_2 (L-H mechanism).

Of all the properties of Au nano-particles responsible for their unique catalytic activity, the low-coordination of Au particle is the most relevant [7].

Although zeolites have been considered as very interesting host materials to disperse Au, because of their pores internal distribution and the possibility of controlling the particle size [4, 12, 13], the CO oxidation reaction has not been experimentally studied in detail using zeolites as support [14, 15]. The theoretical studies of Au supported on zeolites are even scarcer than experimental studies. In fact most of theoretical studies reported are about Au supported on MgO, TiO_2, and Al_2O_3 [7].

Several reactions have been reported using Au supported on different zeolites [3, 4, 13, 16–23]. Silicoaluminophospates (SAPO)-11 has been reported as an interesting material itself and as support in several catalytic reactions [24–35]. One publication was encountered on Au/SAPO-18, over a series of mesoporous and microporous materials containing gold nano-particles to investigate the effects of the host matrix and preparation methods on the properties of gold nano-particles [36]. SAPO-11 has proved to have stability in various reactions endorsed to mild acid sites and desirable pore architecture [28–35], therefore, we consider attractive to study the system Au/SAPO-11. In this work, we present quantum-chemical calculations, using the ONIOM2 method, on gold supported on silicoaluminophospates, SAPO-11, to study CO oxidation reaction. A similar study was reported by us, but in HDS of thiophene [37].

2. Computational Details and Models

All geometry optimizations and energy calculations were performed using the Gaussian-03 program [38]. The lower energy structures were obtained using the two-layer ONIOM2 methodology. For the high-level, [represented by spheres in Fig. 1(a)], DFT approach (B3LYP) with the full-electron 3-21G* basis set for H, C, and O and LANL2DZ with its pseudo potentials for Si, Al, P, were employed. The high-level is composed by 6 tetrahedral, 3 Si, 2 Al, and 1 P, as shown in Figure 1(b). All adsorbed and reactive molecules were included in the high-level. Universal force field approach was employed for the low-level [represented by sticks in Fig. 1(a)]. H atoms were used as boundary atoms in the ONIOM2 calculations.

The SAPO are molecular structures that contain Si—O—Al, P—O—Al, and Si—O—Si but no Si—O—P bonds [Fig. 1(a)] [35, 39, 40]. The model employed in this work has 506 atoms and has been described in previous publications [37, 41]. The bond indexes (BI) were calculated using Wiberg BI in the natural atomic orbital basis approximation. Net charges were calculated according to the Mülliken approach.

Generally, the quality of the results using ONIOM is similar to those computed with periodical calculations [37, 41, 42] and with less computational cost, than did with comparable constrained clusters [43]. Moreover, it has been shown in the literature that the computed adsorption energies with ONIOM method compared well with experimental results [44–47].

3. Results and Discussion

3.1. Au—SAPO-11 AND Au_2—SAPO-11 MODEL

Figure 1(a) displays the molecular structure of Au—SAPO-11 model showing the two levels of

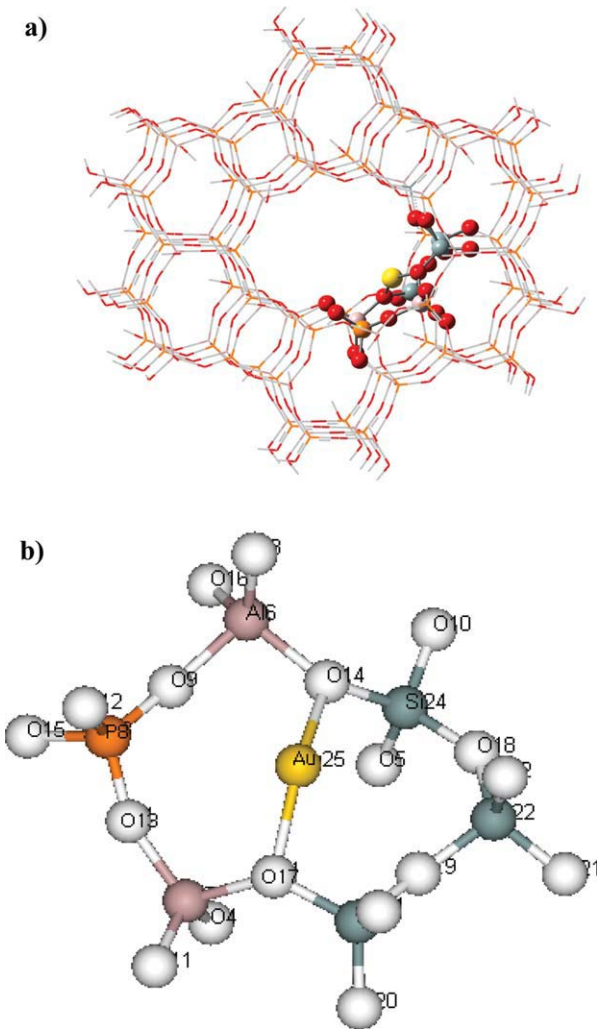

FIGURE 1. (a) Molecular structure used to represent Au—SAPO-11, with the two levels of calculation, high-level highlighted with spheres and low-level represented with sticks. (b) Close view of T6 showing Au interacting with two oxygen in the structure (25 atoms). [Color figure can be viewed in the online issue, which is available at www.interscience.wiley.com.]

calculation. A detail of the high-level, $AuAl_2Si_3PO_{18}$, is shown in Figure 1(b). In this model, the gold formal oxidation state is +1 as has been sufficiently discussed in [37]. To perform calculations with two Au atoms, it is necessary to increase the number of atoms in the high-level, as displayed in Figure 2(a). Figure 2(b) illustrates the Au_2—SAPO-11 model. All geometrical properties and details of theses models are given in [37].

In Au—SAPO-11 model Mulliken charge of au is +0.3. In Au_2—SAPO-11 cluster [Fig. 2(b) and Table I) the Au40 (stronger bonded) has a Mulliken charge of +0.2 and the Au41 (weakly bonded) has a charge of +0.4 (is more oxidized). As it can be seen in Table I Si—O and Al—O bond distances (R) are enlarged specially the last one when passing from SAPO-11 to Au_2—SAPO-11. This fact is confirmed by BI of O1—Al25 and O14—Al4 both diminishes from 0.4 (in SAPO-11) to 0.3 (in Au_2—SAPO-11), whereas R increases. With respect to BA, there is a slight contraction; Si—O14—Al reduces from 150.6 to 137.8° and Si—O17—Al from 140.6 to 136.5°. There is also a rearrangement, as in the Au—SAPO-11 case. In deposing Au41 and Au40, it is observed a slight charge transfer from Au to the bonding oxygen, Au41 and Au40 are oxidized (+0.4 and +0.2, respectively) and the oxygen atoms are reduced (O1 goes from −0.9 to −1.0; O17 from −0.9 to −1.1).

The Au net charges and the relative low Au BI indicate that the Au-support interaction has an important electrostatic component higher than the covalent interaction. However, the Au—Au BI = 0.12 and the Au—Au distance, 3.02 Å, show that there is an inter-metallic interaction between both Au atoms. This Au_2 moiety geometry does not correspond to a ground state Au_2 dimer. Calculation for Au_2 dimer in gas phase show that the Au—Au distance is 2.57 Å and the BI = 1.0 [37].

3.2. CO ADSORPTION ON Au—SAPO-11 AND Au_2—SAPO-11

Gottfried et al. [48] reported that thermal desorption spectra of CO adsorbed on gold (110)-(1 × 2) surface shows at least five desorption states corresponding to desorption energies between 38 and 8 kJ/mol. Goodman and coworkers [49] reported the value of 10.9 kcal/mol for the CO adsorption heat ($-\Delta H_{ads}$) at low-coverage and 7.8 kcal/mol for a coverage > 19% on the same Au surface. CO adsorption on a gold clusters supported on TiO_2 shows a strong dependence of $-\Delta H_{ads}$ with decreasing cluster sizes, with $-\Delta H_{ads}$ in a range of 12.5–18.3 kcal/mol [50].

Fernández and Balbás [51] reported that CO adsorbed on $Au/(Al_2O_3)_{20}$ cluster gives several adsorption energies on different sites. The adsorption site with higher CO binding energy has the CO bond only to the Au atom (Case a). In the cluster case, after CO adsorption, the Au adatom is displaced to form an Al—Au—O bridge with the alumina cluster and the Au—Al to allow the CO molecule to bridge between the Au and the closest substrate oxygen atom. For configuration

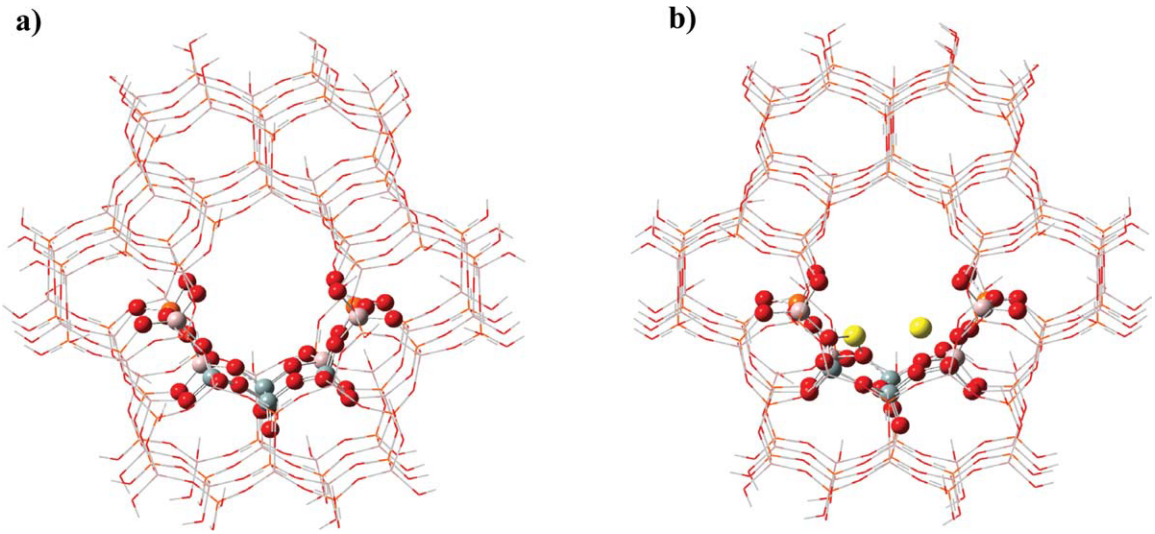

FIGURE 2. (a) Larger high-level model of SAPO-11 structure (39 atoms). (b) Two gold atoms interacting with (a) structure. [Color figure can be viewed in the online issue, which is available at www.interscience.wiley.com.]

b, adsorption of CO occurs at the interface of Au/$(Al_2O_3)_{20}$. For Site c, this isomer configures another top-on-Au adsorption site, with CO more inclined toward the cluster. Adsorption energies are 1.05, 0.74, and 0.64 eV (24.2, 17.1, and 14.8 kcal/mol) for configurations a, b, and c.

Also the adsorption of CO on a Au/Ni(111) surface alloy has been investigated using ab initio density-functional calculations [52]. The lowest adsorption energy of 36 eV (8.3 kcal/mol) is calculated for a CO molecule on top of the Au atom. This is much closed to the experimental adsorption energy on an Au (111) surface of 0.40 eV (9.2 Kcal/mol) [51], and to the value of 0.32 eV (7.4 Kcal/mol) calculated by Gajdos et al. [53].

TABLE I

Relevant bond distances (R) and bond angles of SAPO-11, Au—SAPO-11, Au_2—SAPO-11, CO—Au—SAPO-11 and 2CO—Au_2—SAPO-11. Values corresponding to Au_2—SAPO-11 and 2CO— Au_2—SAPO-11 are in parenthesis.

Bond/Angle	SAPO-11	Au/SAPO-11(Au^2)	CO-Au/SAPO11(Au_2)
R O14—Si	1.61 Å	1.65 Å (1.64)	1.62 Å (1.62)
Si—O14—A1	150,6°	133.3° (137.8)	131.6° (144.4)
R O14—A1	1.68 Å	1.79 Å (1.74)	1.76 Å (1.71)
R O17—Si	1.65 Å	1.66 Å (1.65)	1.69 Å (1.69)
Si—O17—A1	140.6	131.9° (136.5)	127.8° (133.1)
R O17—A1	1.74 Å	1.78 Å (1.80)	1.80 Å (1.84)
Au—Au		(2.98 Å)	(3.12 Å)
Au—O14		2.08 Å (2.36)	2.96 Å (2.21)
Au—O17		2.09 Å (2.29)	2.09 Å (2.57)
O14—Au—O17		146.6°(110.3)	97.1° (106.1)
RO1—Si		(1.68 Å)	(1.67 Å)
Si—O1—A1		(131.1°)	(137.1°)
RO1—A1		(1.80 Å)	(1.79 Å)
RO33—Si		(1.65 Å)	(1.65 Å)
Si—O33—A1		(131.4°)	(138.1°)
RO33—A1		(1.79 Å)	(1.77 Å)
Au—O1		(2.09 Å)	(2.14 Å)
Au—O33		(2.11 Å)	(2.87 Å)
O1—Au—O33		(144.8°)	(164.5°)

Molina and Hammer [54] presented a DFT study on 6-fold coordinated Au atoms in an MgO-supported Au34 cluster and CO reactivity on it. They show different equilibrium structures of adsorbed CO with four different interfaces, CO binding being weaker at edge atoms in direct contact with the substrate, despite of being the lowest-coordinated atoms. The most stable adsorbed CO structures give adsorption energies in the range 0.4–0.5 eV (9.2–11.5 kcal/mol). Several binding configurations of CO at different binding sites with varying coordination: corners, edges, and facets are shown. The binding is 0.2 eV stronger at the corner sites compared with the edge sites.

Recently, Weststrate et al. [55], stated that the CO adsorption for Au (321) and Au (310) show multiple peaks and the calculated desorption energy is 46 ± 6 kJ/mol (0.48 eV or 11 kcal/mol). This value is close to the theoretically predicted value of 0.46 eV for CO adsorption on 6-fold coordinated Au atoms in an MgO-supported Au34 cluster [54].

The CO adsorption energy in Au—SAPO-11 is $\Delta E = -41$ kcal/mol [Fig. 3(a)]. The ΔE is the energy change according to the following reaction:

$$\text{Au—SAPO} - 11 + \text{CO} \rightarrow \text{CO—Au—SAPO} - 11. \quad (1)$$

The CO adsorption energy is defined as:

$\Delta E = E_{\text{CO—Au—SAPO-11}} - (E_{\text{[Au—SAPO-11]}} + E_{\text{CO}})$, where ΔE = is the CO adsorption energy on Au—SAPO-11; and $E_{\text{CO—Au—SAPO-11}}$, $E_{\text{[Au—SAPO-11]}}$, and E_{CO} are the energies of the CO—Au—SAPO-11 aggregate, the Au—SAPO-11, and the free CO.

Gottfried et al. [48] published that desorption of CO gave 5 different states, the highest desorption temperature one (denoted ε) was suggested to correspond to chemisorbed CO (38.4 ± 2.8 Kcal/mol), thus CO adsorption value on Au—SAPO-11 is within the reported value for chemisorbed CO. The adsorption energy change of CO on Au_2—SAPO-11 (2CO—Au_2—SAPO-11) is $\Delta E = -29.7$ Kcal/mol. This aggregate is depicted in Figure 3(b).

Table I summarizes the geometrical properties of CO—Au—SAPO-11. The Au—O14 distance increases from 2.08 to 2.96 Å and O14—Au—O17 angle decreases from 146.6 to 97.1° because of the Au interaction with CO [Figs. 3(a) and 1(b)]. The rest of properties of the substrate remain almost invariable. Au interacts with SAPO-11 producing a geometrical rearrangement evidenced by R and bond angles (BA) changes. Whereas CO interacts with Au on the surface, the SAPO-11 structure remains unaltered.

The charge of Au varies from +0.3 to +0.6 going from Au—SAPO—11 to CO—Au—SAPO-11; it is oxidized on CO adsorption. CO charge changes, going from O, when CO is in gas phase, to −0.33 in adsorbed CO. This fact indicates that there is charge transfer from Au to CO. The Au—CO BI is 0.8 meaning that there is a single bond between the Au and the CO molecule. C26—O27 BI is 2.26 (compared with 2.32 BI C—O

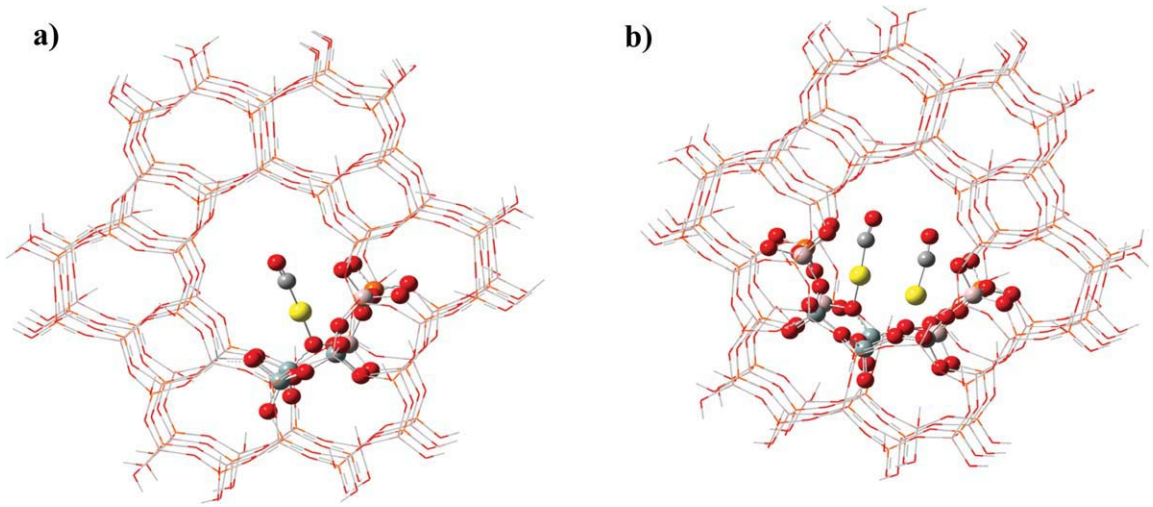

FIGURE 3. CO adsorption: (a) CO adsorbed on Au/SAPO-11; (b) 2CO molecules adsorbed on Au_2/SAPO-11. [Color figure can be viewed in the online issue, which is available at www.interscience.wiley.com.]

in CO gas phase). This fact suggests that the C—O bond character remains after the adsorption. C—O bond distance is 1.16 Å in CO—Au—SAPO-11 (1.15 Å in CO).

The calculated vibrational frequency for carbonyl adsorbed on Au—SAPO-11 is 2113 cm^{-1}. The C—O stretching frequency has been employed to study structure and bonding in transition metal carbonyl complexes and to characterize the active sites of the catalysts. The CO stretching frequency υ_{CO} is susceptible to the molecular surroundings of the bound CO because the extent of backbonding or π-backdonation is significantly altered by the environment. Thus IR spectroscopy of adsorbed CO is an effective method to investigate the electronic states of surface atoms and ions of metals. CO that adsorb on metal atoms and ions interacts with their valence d-electrons, and the frequency of the υ_{CO} stretching vibrations in the surface M-CO complexes depends directly on the effective charge of the adsorbent [56, 57]. Reported frequencies lower than 2080 cm^{-1} have been assigned to CO adsorbed on metallic clusters. The 2119 cm^{-1} frequency, the frequency range 2125–2140 cm^{-1} and the frequency range 2148–2149 cm^{-1}, correspond to $Au^{\delta+}$—CO [14, 56–59]. High-frequencies signals up to 2192 cm^{-1} are assigned to ionic species Au^{+}—CO. Finally weak bands at 2205–2210 cm^{-1} correspond to Au^{+3}—CO [14, 56–59]. The 2113 cm^{-1} is assigned to $Au^{\delta+}$—CO [57].

In Table I geometrical properties of 2CO—Au_2/SAPO-11 cluster are also listed in parenthesis. Au40—O1 and Au40—O33 increase from 2.09 and 2.11 to 2.14 and 2.87 Å, respectively. Au41—O14 and Au41—O17 change from 2.36 and 2.29 to 2.21 and 2.57 Å, respectively. This means that Au40 is bonded to O1 and C42O43, whereas Au41 is bonded to O17 and C44O45. The O1—Au—O33 angle increases from 144.8 to 164.5°. However, O14—Au41—O17 angle remains almost unchanged (110–106°). One CO interacts with each Au, being the SAPO-11 geometrical properties almost unchanged.

Au40 charge changes from +0.2 to +0.4 and Au41charge is +0.41 in Au_2—SAPO-11 and slightly decreases to +0.37 in 2CO—Au_2—SAPO-11. It means that with the CO adsorption the lower oxidation state Au is oxidized. And as mentioned above, each CO adsorbs on the different Au. The charge of CO adsorbed on Au40 changes from 0 to +0.01. The second CO adsorbed on Au41 presents a charge of +0.05. This means that there is a charge transfer from CO to Au41, which is in agreement with the slight reduction of Au41. Because Au40 is oxidized and the CO adsorbed on it has a slightly + charge, the charge transfer is from Au40 to O1 (charge changes from −1.0 to −1.1).

The two C—O BI are 2.26 and 2.24 similar to CO—Au—SAPO-11 model value. The calculated vibrational frequencies for carbonyl adsorbed on Au_2—SAP-11 are 2060 and 2096 cm^{-1} because of CO on metallic Au [56, 57]. These vibrational frequencies calculations are preliminary and seem to suggest that in the two models with 1 Au and 2 Au there is a difference with respect to the CO adsorption. In the first case is an $Au^{\delta+}$—CO type and in the dimer an Au—CO type.

3.3. MODELING OF OXIDATION REACTION OF CO—Au/SAPO-11 AND 2CO—Au_2/SAPO-11

The CO oxidation reaction on CO—Au/SAPO-11 with O_2 is shown in Figure 4(b). The oxidation products are CO_2 and an O atom. The calculated energy change of this reaction is $\Delta E = -52$ kcal/mol with respect to the free systems. The oxidation reaction, we calculate, presents a mechanism of E-R type in which, adsorbed CO reacts with O_2 in gas phase as one of the four mechanisms paths proposed by Shiga and Haruta [11]. These authors considered four types of oxidation pathways: reaction between (a) adsorbed CO and gaseous O_2 (E-R mechanism), (b) adsorbed O2 and gaseous CO (E-R mechanism), (c) adsorbed CO and vicinally adsorbed O2 (L-H mechanism), and (d) adsorbed CO and geminally adsorbed O_2 (L-H mechanism).

No O_2 adsorption was attained on our aggregate. It has been claimed that O_2 molecularly or dissociatively adsorbs on Au when its electric field is negative and the binding energy of oxygen on gold would then increase (partially anionic gold $Au^{\delta-}$). In this case, the dissociative chemisorption of oxygen happens, which opens the pathway to the L-H reactions [6, 60]. The opposite situation favors CO adsorption (partially cationic gold $Au^{\delta+}$). Au25 exhibits a Mulliken charge of +0.6 in consequences CO is adsorbed easily on cationic $Au^{+\delta}$. As it has been mentioned by Hu and coworkers [7] it is clear that CO will interact more strongly than O_2 with gold regardless of the charge on Au. Therefore, they took the calculated O_2 binding energies as a measure of catalytic activity of the free anionic Au_n^- clusters and summarized the literature values of

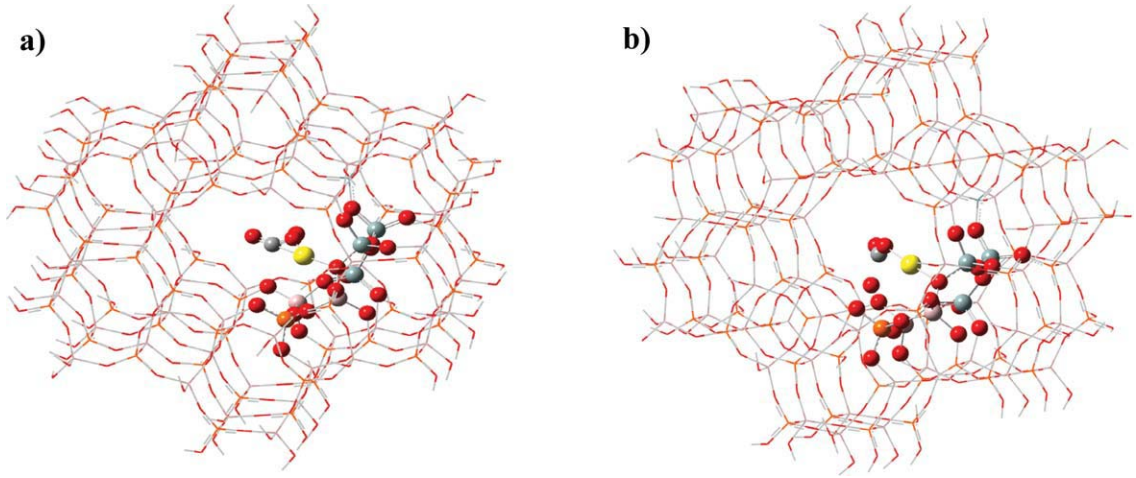

FIGURE 4. CO oxidation reaction on Au/SAPO-11: (a) Start of the reaction; (b) End of the reaction, CO_2 interacting with Au + O. [Color figure can be viewed in the online issue, which is available at www.interscience.wiley.com.]

molecular oxygen adsorption energies from the general results obtained by several groups [61–69]. From these studies, several conclusions have been drawn: (a) negatively charged clusters containing an even number of atoms are more reactive, and bind O_2 more strongly than free neutral clusters. Interestingly, in the case of neutral clusters, an odd number of atoms are found to be more reactive; (b) Only clusters with an odd number of electrons can bind O_2; this appears to be linked to their ability to transfer one electron from an open shell to the molecule, whereas there is no electron transfer from a cationic $Au^{+\delta}$ cluster to O_2.

Analysis of Mulliken charge changes in the transformation from CO—Au—SAPO-11 to CO_2—O—Au/SAPO-11 [Fig. 4(b)], reveled us that Au goes from +0.6 to +0.3 (is reduced) whereas CO is oxidized from −0.07 to +0.37. There is a charge transfer from C to Au and to oxygen. There is almost no change on the substrate, revealing once more that the oxidation reaction is a local phenomenon.

With respect to BI of Au25—O17 raises from 0.2 to 0.3; Au25—O14 changes from 0.1 to 0.02; Au—C26 BI diminishes from 0.8 to 0.02; C26—O27 goes from 2.3 to 1.8; emerges C26—O28 BI = 1.3, C26—O29 BI = 0.6, and Au—O28 BI = 0.3. These modifications explain that Au—O17 in CO—Au/SAPO-11 is slightly stronger than in Au/SAPO-11, whereas Au25—O14 bond breaks; CO triple bond has a BI of 2.3 and changes to CO2 in which C26—O26 has BI 1.8, whereas C26—O28 is lower BI = 1.3, because O28 has an interaction with Au25 also. CO2 separates from Au (consequently Au—C26 BI goes from 0.8 to 0.02).

The oxidation reaction was modeled over 2CO—Au_2/SAPO-11 optimized aggregate as well, and is illustrated in Figures 5(a) and (b). On the left 5a panel, it is observed the initial state of the reaction with the $2O_2$ between the Au—C bond and on the right panel 5b, the oxidation reaction with $\Delta E = -52$ kcal/mol. As shown in Figure 5(b), on the left Au the same oxidation reaction products as with Au/SAPO-11 are obtained. On the right Au, there is also an oxidation reaction but the product is of the carbonate type, which could eventually evolve to CO_2 + O. In Au_2/SAPO-11 as in the case of Au/SAPO-11, there is no O_2 adsorption on Au, therefore we have again an E-R mechanism type, as reported Shiga and Haruta [11] and has already discussed above. However, Norskov and coworkers [70] mentioned two types of mechanism of the CO oxidation over Au nano-particles, in terms of the degree of dependence on the support: (1) a gold-only mechanisms and (2) support induced mechanism. In our model, we have the gold-only mechanism, because we have a local reaction over Au.

In the same way, the study of Mulliken charge changes on the oxidation reaction of 2CO—Au_2/SAPO-11 is specified. Thus, Mulliken charge of Au40 reduces from +0.4 to +0.3 and the charge of Au41 remain unchanged, in the oxidation of 2CO—Au_2/SAPO-11 to (CO_2—O—Au) (CO_3Au)/SAPO-11 [Fig. 5(b)]. While C42 and C44 are oxidized from +0.1 to +0.3, O 43 is reduced from −0.01 to −0.2; O45 is reduced from −0.05 to −0.2.

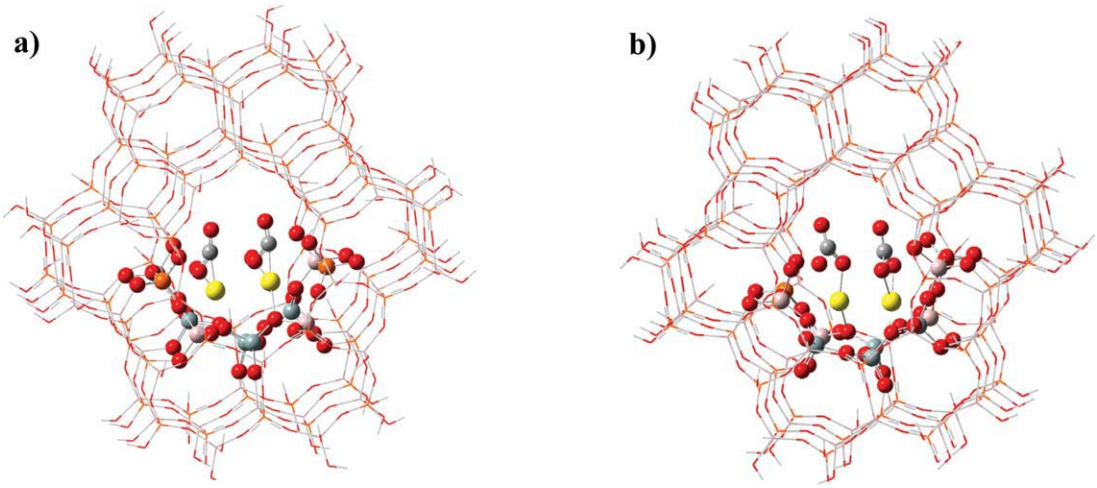

FIGURE 5. CO oxidation reaction on Au_2/SAPO-11: (a) Start of the reaction; (b) End of the reaction, CO_2 interacting with Au + O on the left Au and carbonate type on the right Au. [Color figure can be viewed in the online issue, which is available at www.interscience.wiley.com.]

The rest of O has an average charge of −0.3. There is a slight charge transfer to Au40, but not to Au41. Au41 is linked to the carbonate and to O17 from the substrate. In consequence, the oxidation reaction seems to be restricted to both CO. Once more, it is a local phenomenon.

Concerning BI of main bonds of (CO_2—O—Au) (CO_3Au)/SAPO-11, the remaining Au40—O1 and Au41—O17 retain the 0.2 value of 2CO—Au_2/SAPO-11; Au40—C42 decreases from 0.7 to 0.01 and C42—O43 from 2.3 to 1.8; Au41—C44 reduces from 0.7 to 0.02, and C44—O45 from 2.2 to 1.7. Likewise, C42—O48 and C42—O49 bonds appear with BI = 1.3 and 0.6; C44—O46 and C44—O47 both having BI values of 1.0. These results of BI indicate that Au40 and Au41 are still interacting with O1 and O17; Au40—C42 BI is reduced to 0.01 because of the fact that CO_2 obtained in the oxidation evolves and Au41—C44 BI = 0.02 because of the slight interaction Au41—C44. C42—O43 has a double bond character (in CO_2 BI = 1.9), C42—O48 and C42—O49 bonds appear with BI = 1.3, which is a double bond but O48 has an interaction with Au40 and 0.6 because is an atom O. However, C44—O45 has a double bond character, C44—O46 and C44—O47 present BI = 1.0 as in C—O of HCOOH (BI = 1.01). These BI values confirm the oxidation products CO_2 on Au40 and carbonate on Au41.

In Au_2—SAPO-11 the two Au are different as revealed by geometrical properties and charges, being Au40 the most strongly bonded, and again in 2CO—Au_2/SAPO-11, but in (CO_2—O—Au40) (CO_3Au41)/SAPO-11, Au41—O17 R is 2.11 and Au40—O1 is 2.18 Å. The Mulliken charges of Au40 and Au41 are also different, +0.3 and +0.4, indicating that the two Au behave in a different way. Au40—Au41 R = 2.85 Å. This distance in Au_2/SAPO-11 was 3.02 Å and in 2CO—Au_2/SAPO-11 2.86 Å. BI of Au40—Au41 on Au2/SAPO-11, 2CO—Au_2/SAPO-11 and CO_2—O—Au) (CO_3Au)/SAPO-11 is 0.11, 0.06, and 0.06, respectively. Thus, as it has been already reported by us [37], there is an inter-metallic interaction between both Au atoms.

Conclusions

1. CO adsorption on Au/SAPO-11 is obtained with an energy change difference of ΔE = −41.0 kcal/mol.
2. CO oxidation is produced with an energy change ΔE = − 52.0 kcal/mol. The oxidation reactions modeled in this article exhibits an E-R reaction type mechanism, where gas O_2 reacts with adsorbed CO.
3. A CO molecule is adsorbed in each Au of Au_2/SAPO-11 having an energy change, ΔE = − 29.7 kcal/mol.
4. Both adsorbed CO on Au_2/SAPO-11 are oxidized, ΔE = −52.0 kcal/mol, but in one case Au, CO_2 + O is achieved and in the other one a carbonate is formed.

5. The SAPO-11 could be of great interest as host material for dispersing Au.

References

1. Haruta, M.; Kobayashi, T.; Sano, H.; Yamada, N. Chem Lett 1987, 16, 405.
2. Bond, G. C.; Thompson, D. T. Catal Rev—Sci Eng 1999, 41, 319.
3. Haruta, M. Catal Today 1997, 36, 153.
4. Qu, Z.; Giurgiuy, L.; Roduner, E. Chem Commun 2006, 2507.
5. Molina, L. M.; Hammer, B. Appl Catal A 2005, 291, 21.
6. Fierro-Gonzalez, J. C.; Gates, B. Catal Today 2007, 122, 201.
7. Chen, Y.; Crawford, P.; Hu, P. Catal Lett 2007, 119, 21.
8. Molina, L. M.; Hammer, B. Phys Rev Lett 2003, 90, 206102.
9. Molina, L. M.; Hammer, B. Phys Rev B 2004, 69, 155424.
10. Liu, Z.-P.; Gong, X.-Q.; Kohanoff, J.; Sanchez, C.; Hu, P. Phys Rev Lett 2003, 91, 266102.
11. Shiga, A.; Haruta, M. Appl Catal A 2005, 291, 6.
12. Calzaferri, G.; Leiggener, C.; Glaus, S.; Schurch, D.; Kuge, K. Chem Soc Rev 2003, 32, 29.
13. Mokhtar, M.; Mekkawy, I. J Phys Chem Solids 2003, 64, 299.
14. Tuzovskaya, I. V.; Simakov, A. V.; Pestryakov, A. N.; Bogdanchikova, N. E.; Gurin, V. V.; Farias, M. H.; Tiznado, H. J.; Avalos, M. Catal Commun 2007, 8, 977.
15. Lin, J.-N.; Chen, J.-H.; Hsiao, C.-Y.; Kang, Y.-M.; Wan, B.-Z. Appl Catal B 2002, 36, 19.
16. Wang, A.; Liu, J. H.; Lin, S. D.; Lin, T. S. J Catal 2005, 233, 186.
17. Riach, G.; Guillemot, D.; Polisset, M.; Khodadadi, A. A.; Fraissard, J. Catal Today 2002, 72, 115.
18. Qiu, S.; Ohnishi, R.; Ichikawa, M. J Phys Chem Lett 1994, 98, 2719.
19. Salama, T. M.; Ohnishi, R.; Shido, T.; Ichikawa, M. J Catal 1996, 162, 169.
20. Wang, X.; Wang, A.; Wang, X.; Zhang, T.; Yanga, X. React Kinet Catal Lett 2007, 92, 33.
21. Uphade, B. S.; Akita, T.; Nakamura, T.; Haruta, M. J Catal 2002, 209, 331.
22. Sinha, A. K.; Seelan, S.; Akita, T.; Tsubota, S.; Haruta, M. Catal Lett 2003, 85, 223.
23. Sinha, A. K.; Seelan, S.; Akita, T.; Tsubota, S.; Haruta, M. Appl Catal A 2003, 240, 243.
24. Salehirad, F.; Anderson, M. W. J Chem Soc Faraday Trans 1998, 94, 2857.
25. Yoo, K. S.; Kim, J.-H.; Parkb M. J.; Kim, S. J.; Joo, O. S.; Jung, K. D. Appl Catal A 2007, 330, 57.
26. López, C. M.; Ramirez, L.; Sazo, V.; Escobar, V. Appl Catal A 2008, 340, 1.
27. Sinha, A. K.; Seelan, S. Appl Catal A 2004, 240, 245.
28. Meriaudeau, P.; Tuan, V. A.; Nghiem, V. T.; Lai, S. Y.; Hung, L. H.; Naccache, C. J Catal 1997, 169, 55.
29. Sinha, A. K.; Sivasanker, S. Catal Today 1999, 49, 293.
30. López, C. M.; Guillén, Y.; García, L.; Gómez, L.; Ramírez, A. Catal Lett 2008, 122, 267.
31. Zhang, S.; Chen, S. L.; Dong, P.; Yuan, G.; Xu, K. Appl Catal A 2007, 332, 46.
32. Liu, P.; Ren, J.; Sun, Y. Catal Commun 2008, 9, 1804.
33. Hochtl, M.; Jentys, A.; Vinek, H. J Catal 2000, 190, 419.
34. Machado, F.; López, C. M.; Campos, Y.; Bolívar, A.; Yunes, S. Appl Catal A 2002, 226, 241.
35. Sierraalta, A.; Guillen, Y.; López, C. M.; Martínez, R.; Ruette, F.; Machado, F.; Rosa-Brussin, M.; Soscún, H. J Mol Catal A 2005, 242, 233.
36. Akolekar, D. B.; Foran, G.; Bhargava, S. K. J Synchrotron Radiat 2004, 11, 284.
37. Griffe, B.; Brito, J. L.; Sierraalta, A. J Mol Catal A: Chem 2010, 315, 28.
38. Gaussian 03, Revisión B. 04, Gaussian Inc., Pittsburg, PA, 2003.
39. Machado, F. J.; Lopez, C. M.; Goldwasser, J.; Mendez, B.; Campos, Y.; Escalante, D.; Tovar, M. Zeolitas 1997, 19, 387.
40. Sastre, G.; Lewis, D. W.; Catlow, C. R. A. J Mol Catal A: Chem 1997, 119, 349.
41. Sierraalta, A.; Añez, R.; Ehrmann, E. J Mol Catal A: Chem 2007, 271, 185.
42. Solans-Monfort, X.; Sodupe, M.; Branchadell, V.; Sauer, J.; Orlando, R.; Ugliengo, P. J Phys Chem B 2005, 109, 3539.
43. Fermann, J. T.; Moniz, T.; Kiowski, O.; McIntire, T. J.; Auerbach, S. M.; Vreven, T.; Frisch, M. J. J Chem Theory Comput 2005, 1, 1232.
44. Namuangruk, S.; Pantu, P.; Limtraku, J. J Catal 2004, 225, 523.
45. Namuangruk, S.; Tantanak, D.; Limtraku, J. J Mol Catal A: Chem 2006, 256, 113.
46. Lomratsiri, J.; Probost, M.; Limtraku, J. J Mol Graphics Modell 2006, 25, 219.
47. Jiang, N.; Yuan, S.; Wuang, J.; Qin, Z.; Jiao, H.; Li, Y.-W. J Mol Catal A 2005, 232, 59.
48. Gottfried, J. M.; Schmidt, K. J.; Schroeder, S. L. M.; Christmann, K. Surf Sci 2003, 536, 206.
49. Meier, D. C.; Bukhtiyarov, V.; Goodman, D.W. J Phys Chem B 2003, 107, 12668.
50. Meier, D. C.; Goodman, D. W. J Am Chem Soc 2004, 126, 1892.
51. Fernández, E. M.; Balbás, L. C. J Phys Chem B 2006, 110, 10449.
52. Termentzidis, K.; Hafner, J. J Phys: Condens Matter 2007, 19, 246219.
53. Gajdos, M.; Eichler, A.; Hafner, J. J Phys: Condens Matter 2004, 16, 1141.
54. Molina, L. M.; Hammer, B. Appl Catal A: Gen 2005, 291, 21.
55. Weststrate, C. J.; Lundgren, E.; Andersen, J. N.; Rienks, E. D. L.; Gluhoi, A. C.; Bakker, J. W.; Groot, I. M. N.; Nieuwenhuys, B. E. Surf Sci 2009, 603, 2152.
56. Pestryakov, A.; Tuzovskaya, I.; Smolentseva, E.; Bogdanchikova, N.; Jentoft, F. C.; Knop-gericke, A. Int J Mod Physics B 2005, 19, 2321.

57. Sierraalta, A.; Añez, R.; Diaz, L.; Gomperts, R. J Phys Chem A 2010, 114, 6870.
58. Simakov, A.; Tuzovskaya, I.; Pestryakov, A.; Bogdanchikova, N.; Gurin, V.; Avalos, M.; Farıas, M. H. Appl Catal A: Gen 2007, 331, 121.
59. Pestryakov, A. N.; Bogdanchikova, N.; Simakov, A.; Tuzovskaya, I.; Jentoft, F.; Farias, M.; ıaz, A. D. Surf Sci 2007, 601, 3792.
60. Mc Ewen, J. S.; Gaspard, P. J Phys Chem 2006, 125, 214707.
61. Mills, G.; Gordon, M. S.; Metiu, H. J Chem Phys 2003, 118, 4198.
62. Yoon, B.; Häkkinen, H.; Landman, U. J Phys Chem A 2003, 107, 4066.
63. Häkkinen, H.; Abbet, S.; Sanchez, A.; Heiz, U.; Landman, U. Angew Chem Int Ed Engl 2003, 42, 1297.
64. Kung, H. H.; Kung, M. C.; Costello, C. K. J Catal 2003, 216, 425.
65. Mills, G.; Gordon, M. S.; Metiu, H. Chem Phys Lett 2002, 359, 493.
66. Molina, L. M.; Hammer, B. J Chem Phys 2005, 123, 161104.
67. Ding, X.; Li, Z.; Yang, Y.; Hou, J. G.; Zhu, Q. J Chem Phys 2004, 120, 9594.
68. Okumura, M.; Kitagawa, Y.; Haruta, M.; Yamaguchi, K. Chem Phys Lett 2001, 346, 163.
69. Wells, D. H. Jr.; Delgass, W. N.; Thomson, K. T. J Chem Phys 2002, 117, 1059.
70. Remediakis, I. N.; López, N.; Norskov, J. K. Appl Catal A 2005, 291, 13.